Cathodoluminescence study of ZnO wafers cut from hydrothermal crystals

J. Mass , M. Avella , J. Jiménez , A. Rodríguez , T. Rodríguez , M. Callahan , D. Bliss , Buguo Wang

Física de la Materia Condensada, ETSII, 47011 Valladolid, Spain
Tecnología Electrónica, ETSIT, Universidad Politécnica de Madrid, 28028 Madrid, Spain
Air Force Research Laboratory, Sensors Directorate, Hanscom AFB, MA 01731, USA
Solid State Scientific Corporation, Hollis, NH 03049, USA
Dpto. Matemáticas y Física, UniNorte, Km 5 Barranquilla, Colombia

Abstract

ZnO is a wide bandgap semiconductor with very promising expectation for UV optoelectronics. The existence of large crystals should allow homoepitaxial growth of ZnO films for advanced optoelectronic devices. However, the ZnO substrates are not yet mature. Both defect induced by growth and by polishing together with the high reactivity of the surface are problems to their industrial application. Cathodoluminescence (CL) was used to probe the quality of substrates from two different suppliers. The surface damage was studied by varying the penetration depth of the electron beam, allowing to observe significant differences between the two samples within a 0.5-μm-thick surface layer. CL spectra show a complex band (P1) at ~3.3 eV composed of two overlapped bands (3.31 and 3.29 eV) related to point defects (PD) and the 1-LO phonon replica of the free exciton (FX-1LO). This band (P1) is shown to be very sensitive to the presence of defects and the surface and thermal treatments. Its intensity compared with the excitonic band intensity is demonstrated to provide criteria about the quality of the substrates.

Keywords: A1. Cathodoluminescence; A1. Defects; B1. ZnO bulk

1. Introduction

ZnO is a promising wide bandgap semiconductor for UV optoelectronics, because of its large bandgap (3.4 eV), and large free exciton binding energy (60 meV) allowing room temperature excitonic emission Room temperature heterostructure ZnO light-emitting devices have been recently demonstrated Besides, one of the main potential advantages of ZnO respect to its competitor GaN is the availability of large crystals to be used as substrates for homoepitaxial growth. The high-quality ZnO wafers are expected to boost the progress of commercial ZnO-based devices. However, ZnO wafers machined from ZnO crystals are not yet satisfactory for homoepitaxial growth therefore, other alternative substrates, mainly sapphire, are still preferred. Nevertheless, the achievement of high-quality ZnO wafers is necessary for the breakthrough of high-power ZnO-based devices. In spite of the progress achieved in ZnO crystal growth, (nowadays, high-purity large crystals are available), many issues remain open to improve the wafer quality for homoepitaxial growth. One of the main points concerns the quality of the surfaces, which are very sensitive to machining presenting scratches and subsurface damage due to polishing . On the other hand, the ZnO surfaces are very reactive, oxygen chemisorption being also a relevant issue The result of these phenomena is that the substrate is severely disturbed up to a depth of a few μm A recent work by Cho et al. established a disturbed depth above 4 μm. Accordingly,

the properties of the ZnO substrates for homoepitaxial growth should be determined by the defects proper to the growth process, and the defects induced by polishing and the chemical reactivity of the surface. This means that the improvement of the substrate quality suitable for homoepitaxial growth should address these two aspects; on one side, one should look to upgrade the chemical purity and the control of the native defects in the crystals, and on the other side one should optimize the polishing and the treatments necessary to achieve epiready surfaces.

All this requires a profound knowledge of the defects in ZnO crystals. Luminescence spectroscopy is a powerful technique to study the substrate quality, since it is sensitive to the presence of defects. The high-quality substrates will deliver strong excitonic luminescence emission. The existence of defects should provide additional recombination paths to the e–h pairs, with the concomitant reduction of the excitonic luminescence efficiency. To improve the substrates one needs to understand the role played by native defects and impurities in the luminescence emission, and how they interact in the presence of mechanical damage, and thermal treatments. Cathodoluminescence (CL) is a very powerful tool to study these wafers, because it adds to the luminescence spectroscopy capacity the modulation of the probe depth by varying the energy of the electrons of the excitation beam [9]. We present herein a CL study of different ZnO wafers cut from ZnO crystals grown by the hydrothermal (HTT) method. The main spectral issues concerning the wafer quality are discussed, aiming to establish criteria for wafer quality. The influence of mechanical damage and thermal treatments are also discussed.

2. Experimental setup and samples

The samples were cut from HTT crystals grown at the US Air Force Research Laboratory (AFRL) and Tokyo Denpa (TD). The HTT growth of ZnO crystals is carried out in stainless steel autoclaves using the platinum liners to avoid iron contamination. Large HTT ZnO crystals are usually grown in 2–10 molal alkali solutions at temperatures between 200 and 500 °C and pressures between 500 and 2000 bar [5]. The crystals are grown from parallelepiped seeds with c^+ and c^- basal planes. Typically NaOH, KOH and LiOH mineralizers are used, which is the cause of the high residual alkali impurity concentration. SIMS analysis of the AFRL samples cut directly above the zinc polar face of the seed (c^+ sector) typically revealed traces of Li, 1–10 ppm, K and Na usually not above 1–2 ppm and Al, Fe, Si, C in amounts ranging from 1 to 10 ppm. Plates cut from the oxygen polar face of the seed (c^- sector) present a much higher concentration of impurities ($\approx 5\times - 10\times$), which makes them not suitable for UV device applications. TD sample was not analyzed by SIMS, though this material is known to present much lower impurity concentrations, around one order of magnitude below

Intentional mechanical damage was produced by the-Vickers micro-indentation. Some crystals were annealed in a controlled low-pressure O_2 atmosphere (1.4 Torr, 650 °C, 30 min).

The CL measurements were carried out with a XiCLOne system from Gatan attached to a JEOL 820 Scanning Electron Microscope. CL spectra were acquired at 80 K. The acceleration voltage of the e-beam was varied between 2 and 30 kV, which correspond to probe depths ranging from 100 nm to 4 μm according to the Kanaya–Okayama formula

3. Results and discussion

The typical CL spectrum of ZnO crystal at 80 K is shown in Fig. 1. It consists of a dominant bound excitonic band peaking around 3.36 eV, which consists of several subbands corresponding to excitons bound to different impurities, with the dominant bands being the so-called I4, I6 and I9 excitonic transitions [1,2]; our spectral resolution does not allow to separate them properly; therefore we will treat them as a peak labeled BX; another band, labeled P1, appears at 3.3 eV; a series of bands at lower energy are observed at regular energy intervals of 70 meV, which are phonon replicas of the P1 band; finally, a broad band in the green–yellow spectral range is observed. This spectrum presents significant differences from sample to sample and from face to face [10]. The main differences concern the luminescence efficiency, which is governed by the presence of non-radiative recombination centers (NRRCs), and the relative intensity of the different bands, which is related to the impurities and native defects incorporated during the growth process. In spite of the huge literature concerning the luminescence of ZnO, there are still many uncertainties concerning the origin of the different luminescence bands. The differences between the spectra obtained on different samples evidence that the incorporation of defects is dependent on the growth process, and the growth sector inside the same sample. One observes also that the spectra of some of the samples are shifted to the low energy, which

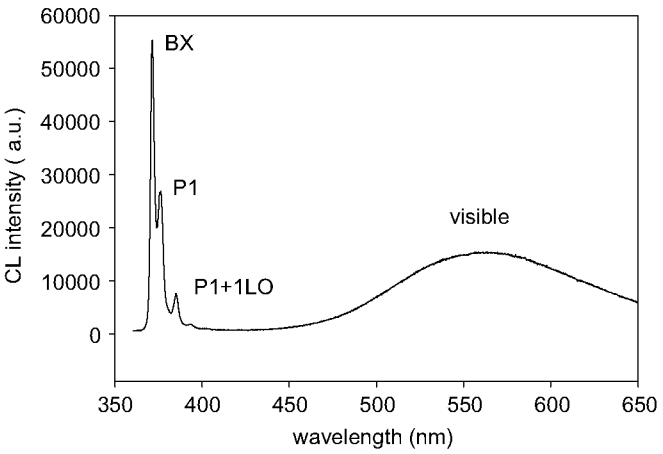

Fig. 1. Typical CL spectrum (80) showing the different bands.

can be interpreted in terms of surface stress and the existence of surface states that are responsible for the self-absorption of the more energetic luminescence photons

This effect is more evident in face Zn, which is softer and the damage induced by polishing is more important than for face O. This effect can be quantified through the Urbach tail, which accounts for surface disorder or surface traps . On the other hand, this tail shows dependence on sample aging. Fig. 2 shows the CL spectra obtained with several month intervals in an AFRL sample, see the shift in the high-energy side and the change in the visible emission, evidencing the reactivity of the surface to the surrounding atmosphere. The surface states are relevant because they can affect the Schottky barriers and the heterojunction band off-sets.

The spectra can be classified according to the excitonic luminescence efficiency, and the relative intensities of the different bands, which reveal differences in the concentration of impurities and intrinsic defects. These differences can arise from the crystal growth process itself, but also from the polishing step The concentration of the NRRCs is higher in the AFRL sample, as deduced from the significantly lower luminescence emission compared with the TD sample. On the other hand, the visible luminescence band in TD sample is very weak, suggesting a low concentration of native defects, and structured, which suggests that it was mostly due to residual Cu impurities

Meanwhile, the visible luminescence of the AFRL sample is more intense and is non-structured, which indicates a higher concentration of native defects, both those acting as NRRCs and those providing visible luminescence. The nature of the NRRCs in ZnO remains

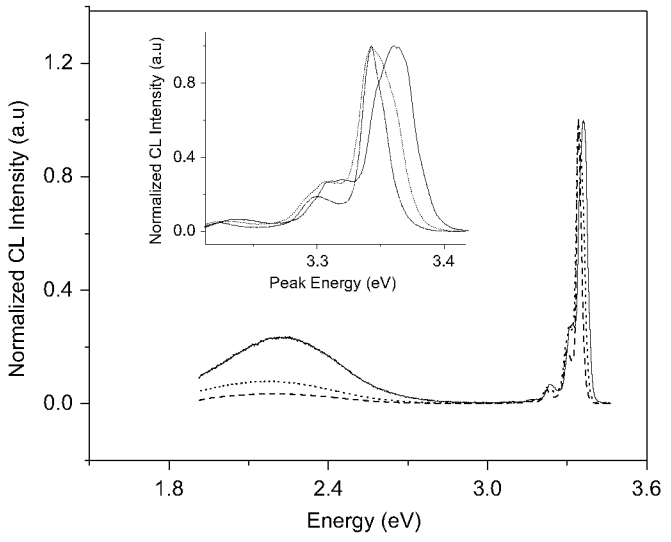

Fig. 2. CL spectra obtained at 80 K and 10 kV e-beam, showing the effect of sample aging in the atmosphere. The three spectra are obtained with 6 months interval period, full line spectrum obtained for the first, dotted line spectrum obtained 6 months later, and dashed line spectrum obtained an additional 6 months later. The inset shows the near band gap spectral region, showing the high-energy photon self-absorption increases with aging.

controversial; Chichibu et al. claimed that the NRRCs are related to V_{Zn} complexes. Extended defects have also been claimed to be responsible for the NRRCs in ZnO crystals. The HTT ZnO has a very low concentration of dislocations ($\approx 10^2\,cm^{-2}$); therefore, if the extended defects are playing a major role as NRRCs, they would be mainly created during polishing, being mostly located close to the surface conforming a death layer; therefore, one should observe differences in the luminescence spectra obtained at different probe depths, i.e. the CL intensity should present a strong dependence with the acceleration voltage of the e-beam.

The CL spectra obtained with different acceleration voltages are shown in Fig. 3 for AFRL and TD samples. The beam current was varied in order to keep constant the e–h pair generation rate in the probed volume. One observes a significant change in the spectra obtained at low voltage with respect to the high-voltage spectra, and significant differences are observed between the samples with changes in the relative intensities of the different peaks, accounting for depth distributions of the defects responsible for the different bands. The AFRL sample shows a very low CL intensity for low-voltage acceleration beam, which evidences a severely damaged surface with very strong nonradiative recombination; for increasing acceleration voltage, the luminescence is enhanced, specially the visible band, which is progressively enhanced up to a depth around 3–4 μm, which should correspond to the region disturbed by polishing and surface chemisorption, in agreement with other reports [4]. One observes a very weak luminescence emission for AFRL sample at low kV, as compared with TD sample, which is due to the better surface preparation of TD sample; the AFRL sample should have a disordered layer close to the surface, around 0.5 μm thick, which is minimized in TD sample. The difference between the two samples is also observed for high kV; the CL intensity of TD sample is more than one order of magnitude higher than the AFRL CL intensity, evidencing that the lower luminescence emission in AFRL sample is not only due to the surface state, but it is also inherent to the growth process, that in the case of AFRL samples introduces a much higher concentration of NRRCs. Note as well the progressive increase of the P1 band for both samples and the strong increase of the visible luminescence emission in the AFRL samples.

The visible luminescence with unstructured bands is usually associated with native defects, either V_O, or O_i and V_{Zn}, for green or yellow bands, respectively [15]. Therefore, the visible luminescence is suitable to monitor the presence of native defects. On the other hand, special attention must be paid to the P1 band, around 3.3 eV, which presents remarkable differences from sample to sample; one observes a strong change in its relative intensity with respect to the BX band for each other sample (see Fig. 3). This strong variability suggests that it could be related to defects. In fact, its origin is a matter of controversy; it has been associated with the first LO phonon replica of the free

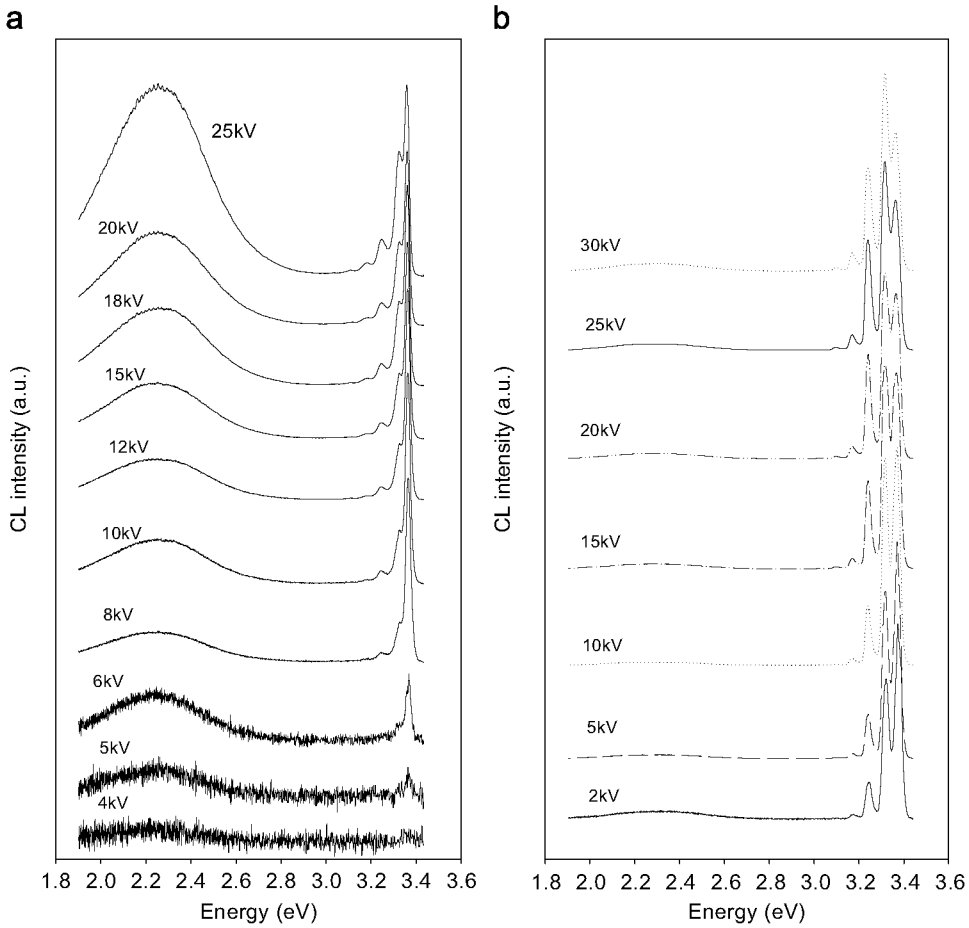

Fig. 3. CL spectra ($T = 80\,\mathrm{K}$, $I_B = 2\,\mathrm{nA}$, Intg. time $= 0.4\,\mathrm{s}$) of AFRL (a) and TD (b) samples obtained for different acceleration voltages of the e-beam. The intensities are normalized.

exciton; it is 72 meV away the FXA exciton peak ; a donor acceptor pair (DAP) transition ; a free to neutral acceptor (e-A°) band ; from an exciton bound to extended defects (dislocations) . Recent results around the Vickers indentations have revealed that this band is complex , and can consist of two subbands overlapping each other, peaking around 3.31 and 3.29 eV, respectively, which were associated with an exciton bound to a point defect, P_D, and the one LO phonon replica of the free exciton, FX-1LO. In general, one observes the convolution of the two bands, which most of the times cannot be separated. Therefore, the intensity and lineshape of the P1 band should depend on the relative weight of the two subbands. In defect-free samples the phonon replica band is the dominant one, then one can expect a strong P1 band because the phonon replica of the excitonic transition is very efficient. In defect-rich regions the excitonic band is quenched and the defect-related band becomes dominant. The defect-related band is clearly observed in mechanically damaged areas, for example, around the Vickers indentations . In AFRL samples the overall P1 is weak, its intensity being much lower than the BX band; however, it can be more intense than BX in mechanically damaged areas, because of the strong quenching of the BX band and the residual emission due to defects, P_D band in this case is dominant. For increasing probe depth it progressively increases, in agreement with the lower contribution of defects far from the surface (Fig. 3). The behavior is different in TD sample, where the P1 band is more intense than the BX band in defect-free areas, but it is relatively quenched in the presence of defects. This also accounts for the observed increase in the relative intensity of the P1 band with increasing acceleration voltage of the e-beam, see Fig. 3, which is due to the improvement of the crystalline quality far from the surface, with the FX-1LO emission dominating the P1 band. This behavior illustrates the possibility to use the P1 band as a test of the sample quality, since it is sensitive to the presence of defects. Therefore, the ratio between the two bands, P1 and BX, should allow to establish a classification of substrates by quality. The best substrates are those with high BX intensity and high I_{P1}/I_{BX} ratio, while a decrease in BX intensity accompanied by a decrease in the I_{P1}/I_{BX} ratio is indicative of lower substrate quality. In regions with high concentration of defects the relative intensity of the P1 band with respect to the BX band can be enhanced, but in this case the BX intensity is very low, which evidences a high concentration of defects;

this situation corresponds to regions with strong mechanical damage due to poor polishing or scratches. These results are summarized in Fig. 4, where one represents the relative intensity I_{P1}/I_{BX} ratio vs. the BX intensity obtained for different samples and facets. The U-shape plot illustrates the above-mentioned quality description, the right arm corresponds to high-quality substrates, while the left arm corresponds to defect rich substrates. Note that defects can be intrinsic, generated during the growth process, or they can be induced by the substrate treatment.

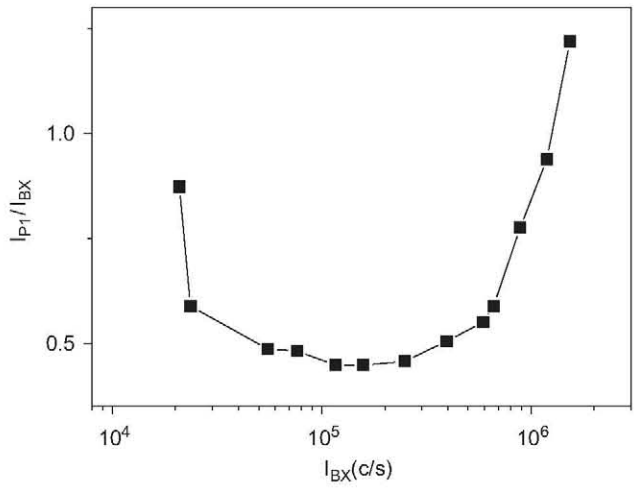

Fig. 4. Plot of the I_{P1}/I_{BX} relative intensity vs. the I_{BX} intensity. The points were obtained over a large number of samples and growth sectors.

Fig. 5 shows the CL image of an indentation area before and after annealing in oxygen atmosphere and the spectra obtained before and after annealing; one observes that the dark areas surrounding the indentation are spread out by the annealing inducing an overall increase of the luminescence intensity, corresponding to the annealing of NRRCs. On the other hand, the spectrum shape is changed by the annealing treatment; there is a relative enhancement of the P1 band, and a shift of the visible luminescence towards the orange yellow region. The green band is quenched by the annealing suggesting that the V_O defects responsible for the green luminescence are removed by the annealing in oxygen atmosphere, while the orange luminescence, associated with either O_i or V_{Zn}-related defects , is enhanced. The evolution followed by the luminescence efficiency and the visible spectra shift suggests that the nonradiative recombination centers could be associated with oxygen-deficient defect complexes rather than V_{Zn}-defect complexes. Further annealing experiments are necessary to understand the nature of the NRRCs in bulk ZnO.

4. Conclusion

The CL of ZnO substrates demonstrate the existence of both bulk and surface defects as responsible for the luminescence efficiency. According to these results, the substrate properties are disturbed up to a depth around 4 μm, which is the consequence of the surface reactivity and the nature of the defects created during crystal growth. The defect-related bands are more sensitive to the surface

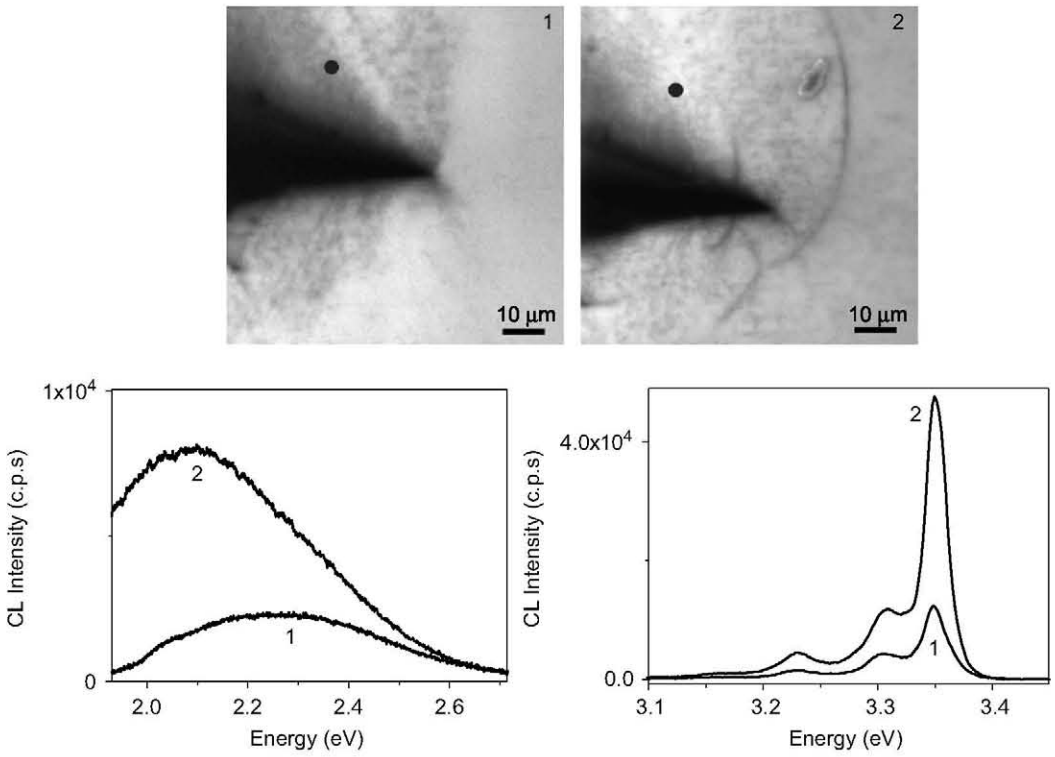

Fig. 5. Panchromatic CL images and spectra (UV and visible ranges) obtained close to the indent (dark dot), before (1) and after annealing (2).

exposure than the excitonic bands. Crystal growth and the subsequent surface polishing determine the luminescence features emitted by the substrates. Mechanical damage and thermal treatments can contribute to restore the properties of the substrates and to understand the nature of the NRRCs in ZnO.

Acknowledgments

The Spanish group was funded by the EOARD (Grant FA8655-04-13073). J. Mass was granted by Alban Program (Grant E03D00117CO). AFRL in Hanscom AFB was funded in part by the Air Force Office of Scientific Research.

References

U. Ozgur, J.I. Alivov, C. Liu, A. Teke, M. Reschikov, S. Douan, V. Avrutin, S.J. Cho, H. Morkoc, J. Appl. Phys. 98 (2005) 041301.
D.C. Look, Semicond. Sci. Technol. 20 (2005) S55.
D.K. Hwang, S.H. Kang, J.H. Lim, E.J. Yang, J.I. Oh, J.H. Yang, S.J. Park, Appl. Phys. Lett. 86 (2005) 222101.
M.W. Cho, C. Harada, H. Suzuki, T. Minegishi, T. Yao, H. Ko, K. Maeda, I. Nikura, Superlatt. Microstruct. 38 (2005) 349.
D. Ehrentraut, H. Sato, Y. Kagamitani, H. Sato, A. Yoshikawa, T. Fukuda, Prog. Cryst. Growth Charact. Mater. 52 (2006) 280.
D.W. Hamby, D.A. Lucca, M.J. Klopfstein, J. Appl. Phys. 97 (2005) 043504.
J.D. Ye, S.L. Gu, S.M. Zhu, F. Qin, S.M. Liu, X. Zhou, L.Q. Hu, R. Zhang, Y. Shi, Y.D. Zheng, J. Appl. Phys. 96 (2004) 5308.
J. Mass, M. Avella, J. Jiménez, M. Callahan, E. Grant III, K. Rakes, D. Bliss, B. Wang, Appl. Phys. A 88 (2007) 95.
K. Kanaya, S. Okayama, J. Phys. D 5 (1972) 43.
J. Mass, M. Avella, J. Jiménez, M. Callahan, E. Grant III, K. Rakes, D. Bliss, B. Wang, MRS Symp. Proc. 878E (2005) Y.1.7.1.
B. Bulakh, L. Khomenkova, V. Kushnirenko, I. Markevich, Eur. J. Appl. Phys. 27 (2004) 305.
H.C. Ong, A.S.K. Li, G.T. Du, Appl. Phys. Lett. 78 (2001) 2667.
N.Y. Garcés, L. Wang, L. Bai, N.C. Giles, L.E. Halliburton, G. Cantwell, Appl. Phys. Lett. 81 (2002) 622.
S.F. Chichibu, T. Onuma, M. Kubota, A. Uedono, T. Sota, A. Tsukazaki, A. Ohtono, M. Kawasaki, J. Appl. Phys. 99 (2006) 093505.
J. Mass, M. Avella, J. Jiménez, M. Callahan, E. Grant III, K. Rakes, D. Bliss, B. Wang, New Materials and Processes for Incoming Semiconductor Technologies, in: S. Dueñas (Ed.), Transworld Research Network, Kerala, India, 2006, p. 113.
T.B. Hur, G.S. Jeen, Y.H. Hwang, H.Y. Kim, J. Appl. Phys. 94 (2003) 5787.
A. Dadgar, A. Krtschil, F. Bertram, S. Giemsch, T. Hempel, P. Veit, A. Díez, N. Oleynik, R. Clos, J. Christen, A. Krost, Superlatt. Microstruct. 38 (2005) 245.
J. Mass, M. Avella, J. Jiménez, M. Callahan, D. Bliss, B. Wang, unpublished.